

Linear temporal interpolation method in ETM+ using MODIS data.

Santiago Ormeño Villajos^a, Marcos Palomo Arroyo^b

Grupo de Investigación de Calidad de Suelos y Aplicaciones Medioambientales - Technical
University of Madrid.

Ctra. de Valencia, km 7.5. 28031, Madrid (Spain).

Email addresses:(^a)santiago.ormeno@upm.es, (^b)marcos.palomo@upm.es

Abstract

The main objective of the present work was to obtain synthetic ETM+ images with improved temporal resolution using MODIS radiometry to expand the applicability of this method to environmental issues that require detailed monitoring over time. To do this, we needed to verify the consistency between the data provided by ETM+ and MODIS.

We used images from these sensors taken on different dates and in different test areas. We designed and validated a spatial resampling method based on statistical parameters and a linear interpolation method for diachronic data.

The results confirm the consistency between MODIS and ETM+ data and their dependence on the spatial variability of the information. They also show that it is possible to obtain images derived from MODIS with the spatial resolution of ETM+ using a simple and robust linear interpolation method. Both results broaden the scope of these sensors' application to environmental issues.

1 Introduction.

Rigorous environmental control requires frequent collection of heterogeneous information about wide areas. In the past, and even today, data were collected by traditional methods based on field measurements. This methodology is slow and expensive and provides a limited sampling rate, especially when studies are carried out across a wide area.

Earth observation satellites equipped with multispectral sensors and an increasing spatial resolution have made it possible to obtain inexpensive, up-to-date, accurate and global environmental information. In this setting, remote sensing techniques are becoming relevant in environmental studies. However, due to the orbital parameter configuration and the recording system's characteristics, it is not possible to simultaneously achieve high spatial, temporal and spectral resolutions in the resulting data.

Enhanced Thematic Mapper Plus (ETM+) and Moderate Resolution Imaging Spectroradiometer (MODIS) are two of the most frequently used sensors in environmental remote sensing studies. ETM+ is a reference sensor that was first used in the early 1980s. It is a medium spatial resolution sensor (30 m in multispectral channels) with a limited temporal resolution (16 days). MODIS is a low spatial resolution sensor (250 - 1000 m) with a high temporal resolution (1 day); thus, it would be advantageous to be able to blend the information from these sensors to create a synthetic document with the spatial resolution of ETM+ and the temporal resolution of MODIS.

Several authors -[1, 2] - have studied the issue of spatial resolution drop. Liang *et al.* [1] have proposed and analyzed a method to retrieve the MODIS surface reflectance from radiometric information given by the ETM+ multispectral temporal resolution bands. They set up a methodology to predict the MODIS surface reflectance using arithmetic expressions and coefficients obtained by adjustment procedures.

Temporal resolution enhancement was analyzed by Gao *et al.* [2], who developed a method to secure the MODIS reflectance at a 30 m spatial resolution based on an analysis of the differences between the sensors.

2 Materials and Methods.

2.1 Spatial imagery.

In the present work, we used both ETM+ and MODIS images. Both sensors are used by many users and their data have been sufficiently validated. In addition, they are mounted on satellites with the same orbital parameters and a temporal delay of 30 minutes during the acquisition of

images; for example, at 10:00 local time in the case of ETM+ and at 10:30 local time in the case of MODIS when the atmospheric disturbances are similar and it is possible to compare these sensors.

Several general characteristics of the sensors are indicated in Table 1.

Table 1: ETM+ and MODIS characteristics.

	ETM+	MODIS
Geometric resolution	15 m - 30 m - 60 m	250 m - 500 m - 1000 m
Radiometric resolution	8 bits	12 bits
Temporal resolution	16 days	1 - 2 days
Spectral resolution	8 bands	36 bands

The ETM+ image values are digital numbers; therefore, it was necessary to transform them into radiance values and surface reflectance prior to comparison with the MODIS reflectance data. In the present work, only red and near-infrared spectral bands were considered because of their importance in environmental studies and the higher level of spatial resolution of MODIS in these bands. Surface reflectance was computed by applying calibration coefficients and using the equation of Markham and Baker [3], and the atmospheric correction was carried out using the *Dark Object Subtraction* method [4].

The MOD09GQ standard product of MODIS provides an estimation of the spectral reflectance at ground level, without being affected by atmospheric dispersion and absorption. The algorithms applied to the data taken by the sensor, together with the auxiliary data necessary for performing the atmospheric correction, are detailed in [5].

2.2 Linear temporal interpolation method.

In order to obtain the high temporal and spatial resolution images, an interpolation method that considers time-variant differences for reflectance values is proposed; this allows us to obtain an interpolated synthetic image with temporal variation information gained from two ETM+ and MODIS images of similar dates, with the assumption of linear variation in a time interval.

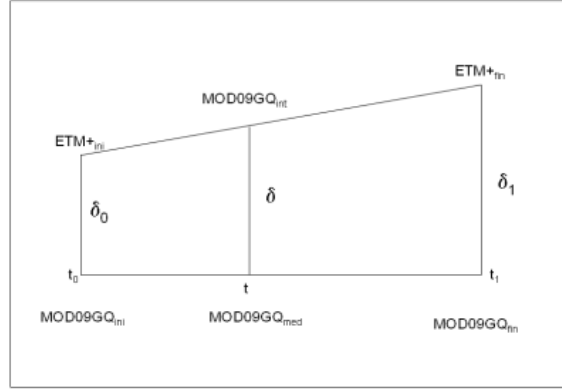


Figure 1: The proposed temporal interpolation method.

As deduced from Figure 1, the value of δ was obtained from the expression:

$$\delta = \frac{\delta_1 - \delta_0}{t_1 - t_0} t + \delta_0 \quad (1)$$

where δ_0 and δ_1 are the differences between the surface reflectance calculated from ETM+ and that provided by the MOD09GQ product. t_0 and t_1 are the initial and final dates, respectively, expressed in days, and t is the intermediate date of the desired interpolation.

Because reflectance variations in time are caused by multiple factors, the linear assumption is more accurate when the time interval between the dates of the initial and final images is smaller.

2.3 Characteristics of the study area.

For the purpose of this work, we needed two ETM+ images from similar dates, the MODIS images for the same dates, and an intermediate MODIS image. To validate the results, we used an intermediate ETM+ image taken simultaneously with the MODIS one.

The selected images were obtained in part of the USA, bounded by the UTM15-WGS84 coordinates: (771000, 4000930) upper left corner and (817920, 3971020) lower right corner. This area was selected because the area includes croplands of relatively small size compared to the MODIS pixel size, urban areas, rivers and native vegetation and a non-linear reflectance variation in a river bed by flooding.

The dates of the images were 11/14/2001, 12/24/2001 and 02/02/2002. For each date, an ETM+ image and a MODIS image were available. To conduct a pixel-to-pixel analysis, MOD09GQ data were resampled to match a 30-m resolution. Some of the images are shown in Figures 2 and 3.

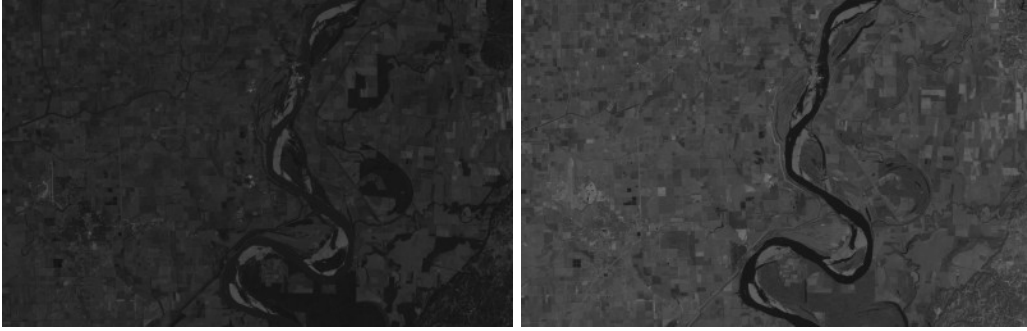


Figure 2: Zone of analysis. Bands 3 & 4 of ETM+ image (14/11/2001).

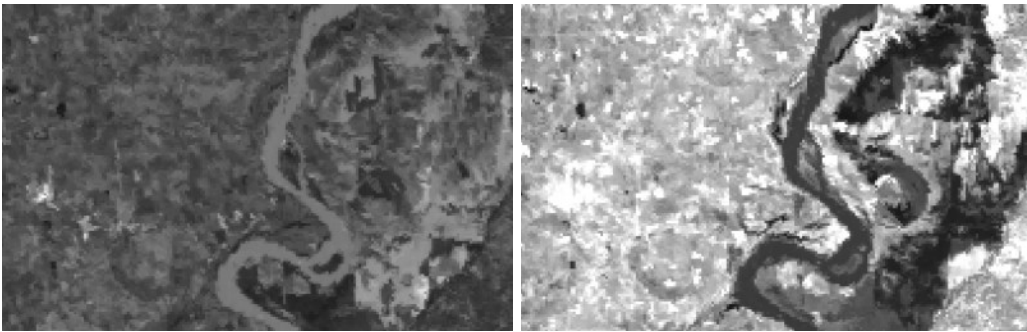


Figure 3: Bands 1 & 2 of MOD09GQ, resampled at 30m. (24/12/2001).

3 Results and Discussion.

We wanted to obtain a 30-m spatial resolution synthetic image from the MOD09GQ standard product (surface reflectance) with a 250-m spatial resolution and 1-day temporal resolution, extracting radiometric information provided by the ETM+ sensor, which would allow the daily surface reflectance to be determined.

All data sets, obtained in different dates, had to be registered and matched pixel to pixel. To geo-reference the ETM+ images, we used metadata, and the result was validated with the NASA World Wind Tool [6]. The MODIS Reprojection Tool was used to change the projection and select the study area in the MODIS images.

As a first assumption, we formulated a constant difference between the ETM+ and MODIS pixel values. Starting with a MODIS image (previously resampled to 30 m) and an ETM+ image from the same initial date, the differences were computed. To obtain a synthetic image for an intermediate date, the differences were added to MOD09GQ (Figure 4). The ETM+ image corresponding to this last date was used to validate the results.

Adding up the differences resulted in negative pixel values. Because these are not allowed as values for reflectance, they were set to 0.000. Such values only represent 2.5% of all pixels.

The differences between the synthetic and control images are shown in Table 2. In this table, B1 and B3 are the red bands in MODIS and ETM+, and B2 and B4 are near-infrared bands for these sensors. The *s* suffix indicates a *synthetic* image.

Table 2: Differences between the synthetic image (BxS) and ETM+ (EBx) reflectance in reflectance values, for each band.

	B1S-EB3 (reflectance)	B2S-EB4 (reflectance)
Maximum	0.4313	0.5345
Minimum	-0.5563	-0.8875
Average	-0.0070	0.0021
Std. Dev.	0.0283	0.0510

Table 3 shows the correlation between the synthetic image generated from MOD09GQ and the control ETM+ image.

Table 3: Correlation coefficient between the synthetic image (BxS), the control ETM+ image (EBx) and the original MODIS image (MBx).

	B1S	EB3	B2S	EB4
EB3	0.56	1.00	-	-
MB1	0.56	0.57	-	-
EB4	-	-	0.72	1.00
MB2	-	-	0.76	0.69

The analysis of this table shows that this constant interpolation method does not improve the correlation between MODIS 30 m and ETM+. The correlation coefficients remain constant in the original MODIS image and the synthetic image.

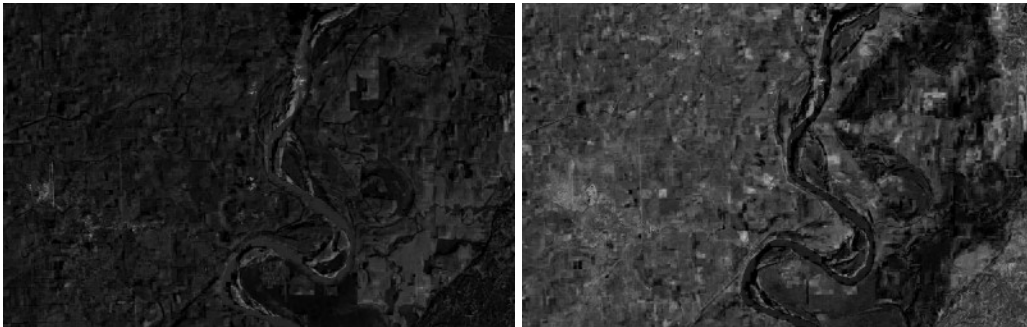


Figure 4: Generated synthetic image (bands 1 & 2)

The assumption of constant reflectance differences in time between MODIS and ETM+ is not correct. This could be due to the influence of heterogeneous pixels, whose reflectance values are determined by integrating multiple objects with different radiometric properties and diachronic behavior and by the temporal evolution of the cover types presents in the images (suchs as natural vegetation or crops).

All computations and processes were carried out with the SOVMAP software, created by the authors and which allows data acquired from both sensors to be imported and treated. An automated process was saved in the SOVMAP Modelling Language for retrieval at a later date

Firstly, the surface reflectance is calculated from the initial and final ETM+ images, and then it is possible to obtain differences between this value and the MOD09GQ result. Using these values and the differences corresponding to the intermediate MODIS image and the application of (1), the interpolated image is obtained.

To validate the process, we used an ETM+ image for an intermediate date to compare reflectance values of the synthetic image. Negative values were set to 0.000.

The statistics of the synthetic image (noted by s index), the control ETM+ image (with the E prefix) and the MOD09GQ (with prefix M) document are shown in Tables 4 and 5, for the selected bands.

Table 4: Comparison of synthetic (BxS), ETM+ (EBx) and original MOD09GQ (MBx) images statistics with the proposed method, in reflectance values.

	B1S (re- flectance)	EB3 (re- flectance)	MB1 (re- flectance)	B2S (re- flectance)	EB4 (re- flectance)	MB2 (re- flectance)
Maximum	0.3704	0.7323	0.2148	0.4722	0.9826	0.4557
Minimum	0.0000	-0.0164	-0.0189	0.0000	-0.0404	0.0136
Average	0.0659	0.0674	0.0743	0.1252	0.1256	0.1322
Std. Dev.	0.0269	0.0268	0.0202	0.0592	0.0709	0.0550

Table 5: Correlation coefficient between the synthetic image (BxS) and the initial ETM+ (EBx) and MODIS (MBx) images.

	B1S	EB3	B2S	EB4
EB3	0.72	1.00	-	-
MB1	0.69	0.57	-	-
EB4	-	-	0.84	1.00
MB2	-	-	0.82	0.69

As shown in Table 5, an improvement in the correlation between the synthetic document and ETM+ is achieved with the last proposed interpolation method. The average and standard deviation also show this improvement, so the interpolated image is more closely related to the control ETM+ image than to the MODIS resampled image. The correlation coefficients are 0.72 in the Red band (bands 1, MODIS and 3, ETM+) and 0.84 in the NIR band (bands 2, MODIS and 4, ETM+), compared to 0.57 and 0.69 for the initial documents.

Differences between the synthetic and control images are shown in Table 6 in reflectance values. Calculated values for reflectance are similar to those obtained by Gao *et al.* [2] and are of the same order of magnitude or even better.

Table 6: Differences between the synthetic image (BxS) and ETM+ (EBx) reflectance, in reflectance values.

	B1S-EB3 (reflectance)	B2S-EB4 (reflectance)
Maximum	0.2220	0.3392
Minimum	-0.4660	-0.9120
Average	-0.0015	-0.0006
Std. Dev.	0.0199	0.0393

Figure 5 shows the synthetic document obtained by this interpolation method.

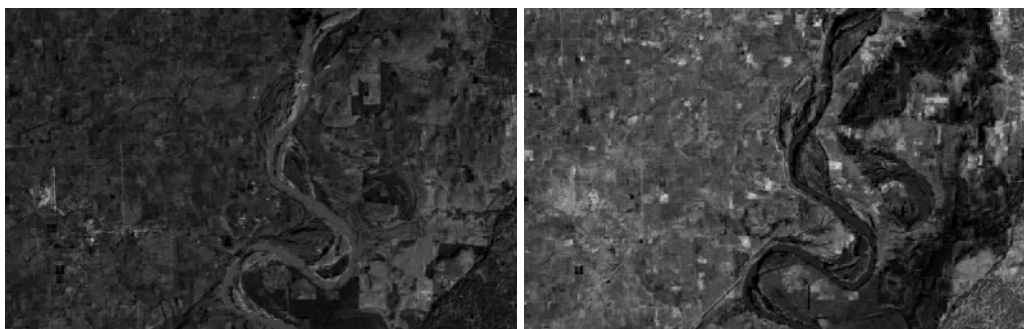


Figure 5: Image obtained by interpolation (bands 1 & 2).

Figure 6 displays a detail of an area in the original MODIS image and the interpolated image. This is a sample of the improvement achieved by the interpolation procedure. In addition to the better correlation coefficient, this improves the interpretation of details and feature enhancement.

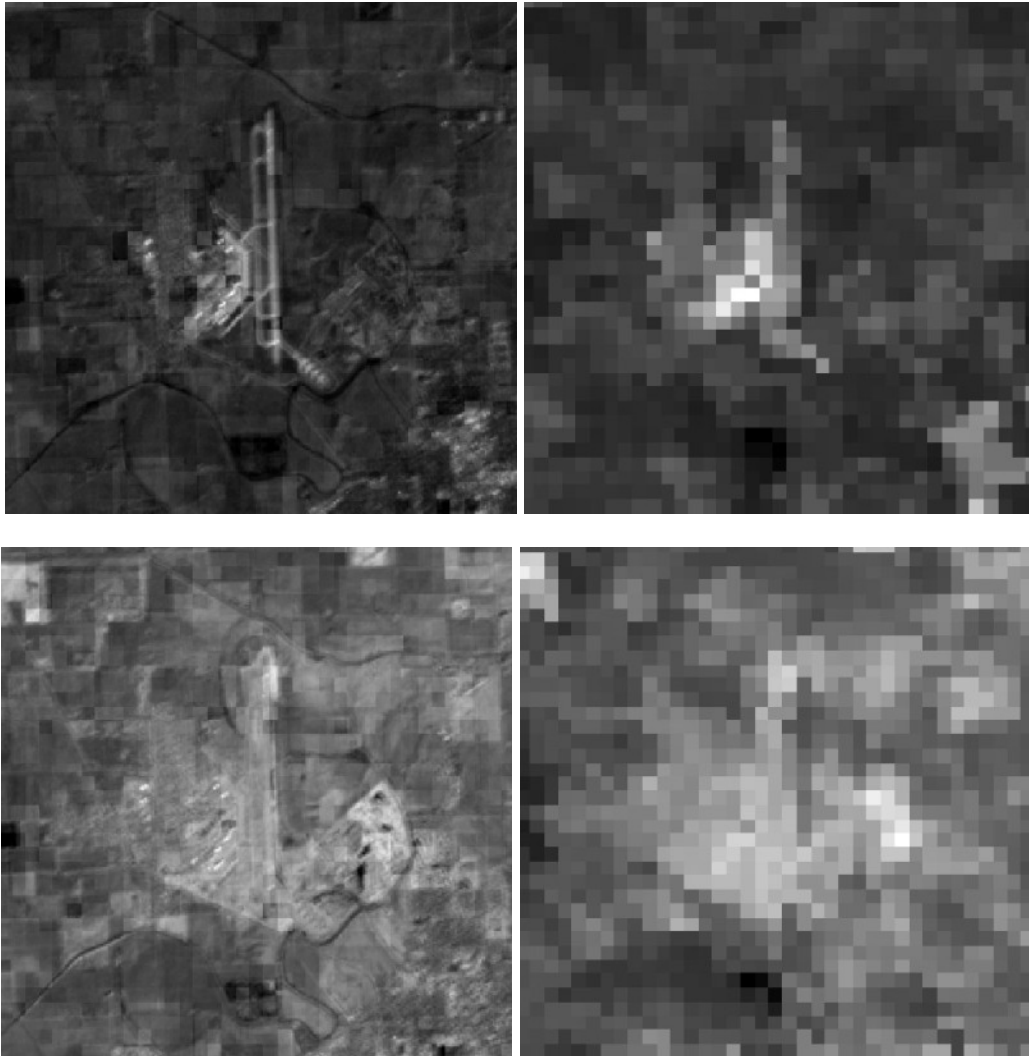


Figure 6: Detail of the interpolated image (at the left), compared with the original one (at the right). (B1 top; B2 bottom). (B1, top; B2, bottom).

In the analysis of the spatial distribution of differences, the worst results are observed in roughly spatially variable areas and where there is a non-linear change between the initial and final images (e.g., a river bed) because the interpolation method only works well when there is linear variation between the images (Figure 7).

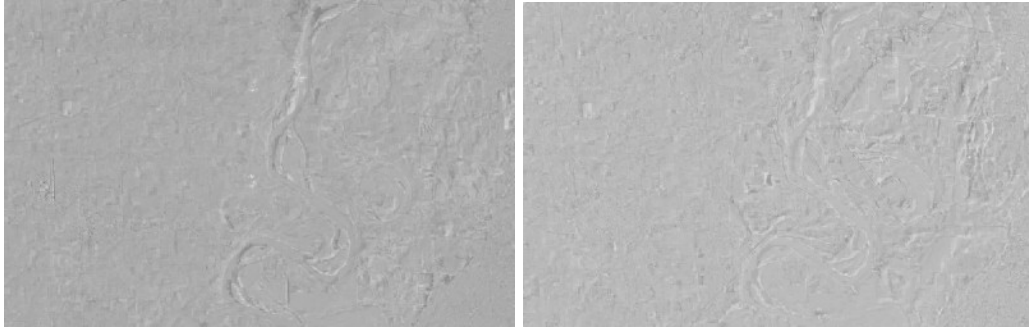


Figure 7: Differences between the synthetic image and the ETM+ verification image (bands 1 & 2). (Dark grey, shows low differences and light grey, shows high differences)

Figure 8 shows a sample of non-linear variation in time disrupting the interpolation results. In this case, the breakdown is due to an abrupt change in the river level occurring sometime between the initial and the intermediate images and continuing through the final image. This phenomenon produces bad interpolation results.

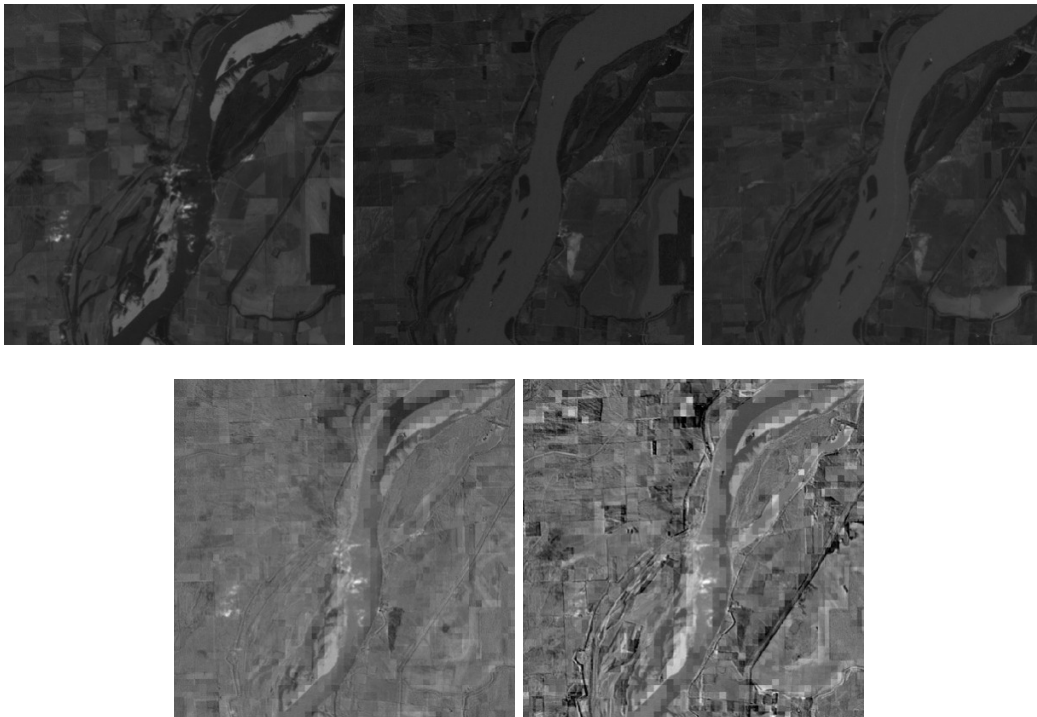


Figure 8: Non-linear variations and effect on interpolation.

To avoid this, we carried out a separate analysis of interpolation accuracy. For this purpose, we selected four zones in the original image, taking into account land take and spatial variability criteria (Figure 9):

- Zone 1. Mainly crop lands.

- Zone 2. Crop lands and urban area.
- Zone 3. Mainly native vegetation.
- Zone 4. Crop lands and native vegetation.



Figure 9: Selected zones of analysis, in the ETM+ image, from left to right: Zone 1, Zone 2, Zone 3 and Zone 4.

The tables 7,8,9 and 10, shows the statistics regarding the differences between the synthetic and the control ETM+ images and the correlation coefficients for each zone.

Table 7: Zone 1. Statistics of differences and correlations between the interpolated (BxS) and control image (EBx) for the two bands considered.

	B1S-EB3 (reflectance)	B2S-EB4 (reflectance)
Maximum	0.0908	0.3392
Minimum	-0.2226	-0.2491
Average	-0.0064	-0.0067
Std. Dev.	0.0160	0.0319

	B1S	EB3	B2S	EB4
EB3	0.60	1.00	-	-
MB1	0.58	0.39	-	-
MB4	-	-	0.74	1.00
MB2	-	-	0.65	0.42

Table 8: Zone 2. Statistics of differences and correlations between the interpolated (BxS) and control image (EBx) for the two bands considered.

	B1S-EB3 (reflectance)	B2S-EB4 (reflectance)
Maximum	0.2175	0.2298
Minimum	-0.4616	-0.4323
Average	-0.0058	-0.0046
Std. Dev.	0.0215	0.0340

	B1S	EB3	B2S	EB4
EB3	0.75	1.00	-	-
MB1	0.62	0.45	-	-
EB4	-	-	0.80	1.00
MB2	-	-	0.72	0.53

Table 9: Zone 3. Statistics of differences and correlations between the interpolated (BxS) and control image (EBx) for the two bands considered.

	B1S-EB3 (reflectance)	B2S-EB4 (reflectance)
Maximum	0.1090	0.1594
Minimum	-0.1559	-0.1960
Average	-0.0008	0.0011
Std. Dev.	0.0231	0.0380

	B1S	EB3	B2S	EB4
EB3	0.79	1.00	-	-
MB1	0.69	0.55	-	-
EB4	-	-	0.84	1.00
MB2	-	-	0.88	0.80

Table 10: Zone 4. Statistics of differences and correlations between the interpolated (BxS) and control image (EBx) for the two bands considered.

	B1S-EB3 (reflectance)	B2S-EB4 (reflectance)
Maximum	0.0769	0.2581
Minimum	-0.0825	-0.3646
Average	0.0035	-0.0031
Std. Dev.	0.0185	0.0576

	B1S	EB3	B2S	EB4
EB3	0.72	1.00	-	-
MB1	0.69	0.51	-	-
EB4	-	-	0.76	1.00
MB2	-	-	0.85	0.65

Table 11: Increase in the correlation coefficient between the synthetic image and the control image for the different zones, for each band.

	$\Delta\rho$ B1	$\Delta\rho$ B2
Zone 1	0.21	0.32
Zone 2	0.30	0.27
Zone 3	0.24	0.04
Zone 4	0.21	0.11

A study of Table 11 shows that major improvements are achieved with interpolation in zones 1 and 2 because of the high spatial variability and limited resolution of MODIS to register small details. In zones 3 and 4, this improvement is less noticeable due to the reduced spatial variability.

We also studied the influence of land cover type. For this purpose, we performed an unsupervised classification of the initial ETM+ image using the maximum likelihood model, creating five classes: *Water* (W), *Sand* (S), *Native Vegetation* (NV), *Light Bare Soil* (BS I) and *Dark Bare Soil* (BS II). The results of the classification are shown in Figure 10.



Figure 10: Classified image. Land cover types are *Water* (W), *Sand* (S), *Native Vegetation* (NV), *Light Bare Soil* (BS I) and *Dark Bare Soil* (BS II).

Due to the increased river flow, the sand in the river bed disappears in the images for the intermediate and final dates.

The spectral signatures of the five selected classes are shown in Figure 11.

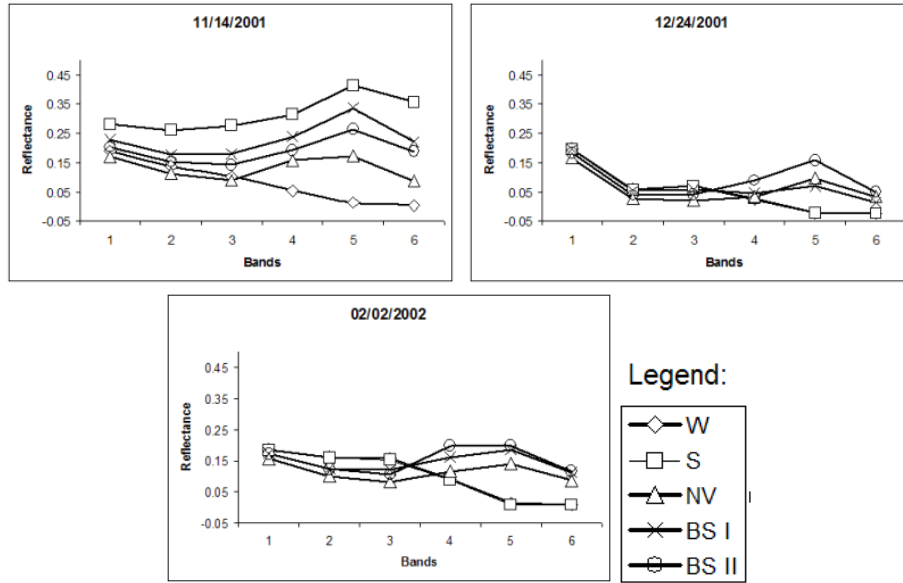


Figure 11: Spectral signatures of the three selected dates. (*Water (W)*, *Sand (S)*, *Native Vegetation (NV)*, *Light Bare Soil (BS I)* and *Dark Bare Soil (BS II)*).

The statistics on the differences between the synthetic and the control ETM+ images are shown in Table 12. The image had already been classified when the statistics were calculated

Table 12: Analysis of differences by domain class. Bands 1 & 2 .

B1S-B3 (reflectance)	W	S	NV	BS I	BS II
Maximum	0.0774	0.1081	0.0727	0.1178	0.0928
Minimum	-0.1027	-0.1197	-0.1266	-0.1609	-0.1233
Average	-0.0112	0.0178	-0.0004	-0.0007	-0.0043
Std. Dev.	0.0261	0.0285	0.0182	0.0193	0.0180
B2S-B4 (reflectance)	W	S	NV	BS I	BS II
Maximum	0.1244	0.1571	0.2004	0.2092	0.2024
Minimum	-0.2157	0.1287	-0.1931	-0.2130	-0.3051
Average	0.0008	0.0171	0.0056	0.0004	-0.0070
Std. Dev.	0.0359	0.0504	0.0356	0.0385	0.0412

From the table above, we can state that the results are similar to those of Table 6, except in the 'Sand' class, which shows slightly worse results because this class disappears when the river flow increases.

4 Conclusions.

The proposed interpolation method improves the spatial resolution for synthetic interpolated images starting from ETM+ data sets. This is because the correlation coefficient increases in every analyzed assumption. This allows us to obtain multispectral images with a temporal resolution

of one day and a spatial resolution equal to ETM+, thereby expanding the applicability of the MODIS sensor.

Obtaining reflectance differences with linear interpolation has improved the correlation between synthetic MODIS and control ETM+, in contrast to the assumption of constant differences in time. Moreover, it is a simple method that could be implemented to obtain systematic interpolated images with 30 m spatial resolution and 1 day temporal resolution.

It is showed that it is possible to improve the spatial resolution of MODIS with two ETM+ images taken on similar dates by means of linear interpolation in differences between pixels using a simple method that provides results similar to those obtained by Gao *et al.* [2], but easier to implement.

In conclusion, it is possible to use the MODIS sensor to obtain environmental parameters suitable for application in a wider range of scales than previously thought, as long as a synthetic image of 30 m of spatial resolution can be used in studies at smaller scales.

References

- [1] S. Liang, H. Fang, M. Chen, C. Shuey, C. Walthall, C. Daughtry, J. Morisette, C. Schaaf, A. Strahler, Validating modis land surface reflectance and albedo products. methods and preliminary results, *Remote Sensing of Environment* 83 (1) (2002) 149–162.
- [2] F. Gao, J. Masek, M. Schwaller, F. Hall, On the blending of the landsat and modis surface reflectance: predicting daily landsat surface reflectance, *Geoscience and Remote Sensing, IEEE Transactions on* 44 (8) (2006) 2207–2218.
- [3] B. L. Markham, J. L. Barker, Landsat mss and tm post-calibration dynamic ranges, exoatmospheric reflectances and at-satellite temperatures, *EOSAT Landsat Technical Notes* 1 (1986) 3–8.
- [4] P. Chavez, Radiometric calibration of landsat thematic mapper multispectral images, *Photogrammetric Engineering and Remote Sensing* 55 (1989) 1285–1294.
- [5] E. F. Vermote, A. Vermeulen, Atmospheric correction algorithm: Spectral reflectances (mod09), modis atbd, Dept. of Geography, University of Maryland.
- [6] C. Maxwell, R. Kim, T. Gaskins, F. Kuehnel, P. Hogan, Nasa’s world wind, <http://worldwind.arc.nasa.gov> (2007).
URL <http://worldwind.arc.nasa.gov/>